Reactive Interference Management for Radio Astronomy in Radio Dynamic Zones Using ASTRA

Aarushi Sarbhai*, David Johnson*, Kirk Webb*, Leigh Stoller*, Oren Collaco†, Alex Orange*, Samuel Zachary*,
Bo Pearce†, Serhat Tadik‡, Sylvia Llosa†, Arvind Aradhya†, Alexander Pollak¶, Wael Farah¶,
Jacobus Van der Merwe*, Kevin Gifford§, Neal Patwari*, Gregory Durgin‡, David DeBoer§, Sneha Kasera*
*Kahlert School of Computing, University of Utah
†Department of Computer Science, University of Colorado Boulder
‡School of Electrical and Computer Engineering, Georgia Institute of Technology
§Radio Astronomy Lab, University of California at Berkeley
¶Science and Engineering Operations, SETI Institute

Abstract—Radio Dynamic Zones (RDZs) enable diverse spectrum-sharing scenarios, including advancing coexistence between active and passive spectrum users. We consider RDZs where radio astronomy coexists with active transmitters and introduce the Adaptive Spectrum Tuning and Reactive Allocation (ASTRA) framework, used by a Zone Management System to manage spectrum access to transmitters. We develop and deploy the first RDZ testbed at a radio astronomy facility, the Hat Creek Radio Observatory, to demonstrate a practical solution for managing interference from active transmitters to radio telescopes in over-the-air experiments. To comprehensively evaluate our approach, we simulate RDZs of varying sizes and demonstrate that ASTRA maintains interference at the radio telescopes below acceptable thresholds while maximizing spectrum access to transmitters in the zone.

Index Terms—Zone Management System, Sensitive Passive Receiver, Radio Dynamic Zone Testbed

I. Introduction

Wireless spectrum regulatory agencies, such as the Federal Communications Commission (FCC) and National Telecommunications and Information Administration (NTIA), are propelling spectrum-sharing initiatives in underutilized radio frequency bands [1]–[4]. These initiatives enable opportunistic access for additional users to meet the growing spectrum demand. Radio Dynamic Zones (RDZs) have been proposed to enable diverse spectrum-sharing scenarios, including supporting experimentation to advance coexistence between active and passive spectrum users [5]. RDZs can be leveraged to increase spectrum utilization [4] by supporting commercial, scientific, and experimental users, including radio astronomy [6], [7].

Radio Astronomy Service (RAS), a passive spectrum user, relies on detecting faint extraterrestrial signals and is highly susceptible to terrestrial interference. Radio telescopes are highly sensitive and observations span wide frequency ranges, making them vulnerable to interference, even from sources up to 100 km away. Historically, RAS relied on exclusive access to some crucial frequency bands and geographic isolation enforced by Radio Quiet Zones prohibiting transmissions [8]. However, this approach is becoming unsustainable due to expanding wireless deployments [9].

In this paper, we consider RDZs where passive RAS coexists with active transmitters, such as cellular and experimental users. These transmitters may be mobile and operate for durations ranging from minutes to years. The key challenges to enable coexistence are: (1) Operational parameters of RAS are often not known in advance, making computationally intensive transmitters scheduling infeasible. If interference is detected by RAS, immediate mitigation actions are needed. (2) Spectrum allocation must scale with transmitter density and adapt to dynamic changes in the zone. (3) Accurately modeling aggregate signal propagation remains an open problem. These challenges underscore the need for an adaptive spectrum management solution.

We introduce the Adaptive Spectrum Tuning and Reactive Allocation (ASTRA) framework, used by a Zone Management System (ZMS) to enable spectrum sharing between radio astronomy telescopes and transmitters within the RDZ, as shown in Figure 1. Real-time interference detection at RAS facilities, often via spectrum monitors [10]–[12], alerts the ZMS about harmful interference. The ZMS responds by revoking spectrum access for select transmitters. Once interference subsides, spectrum is reassigned to some transmitters and transmission power is gradually increased. Through this iterative process, ASTRA identifies the allocation configuration that protects the telescopes while optimizing spectrum utilization.

Reactive interference management is not necessarily novel. Our prior work [6] introduced a basic reactive framework for spectrum sharing between dynamic RDZs and satellite sensing stations. Although effective for satellite receivers, the basic approach is inadequate for RAS, which has higher sensitivity and requires faster mitigation due to shorter observation sessions. Furthermore, interference identification methods differ significantly. These unique requirements necessitate substantial modifications and extensions to the basic reactive framework.

ASTRA differs from the basic framework in several significant ways. First, the basic framework relied on binary on/off control of secondary spectrum access. ASTRA enables fine-grained control by dynamically adjusting transmit power. Second, allocations of new transmitters are based on expected
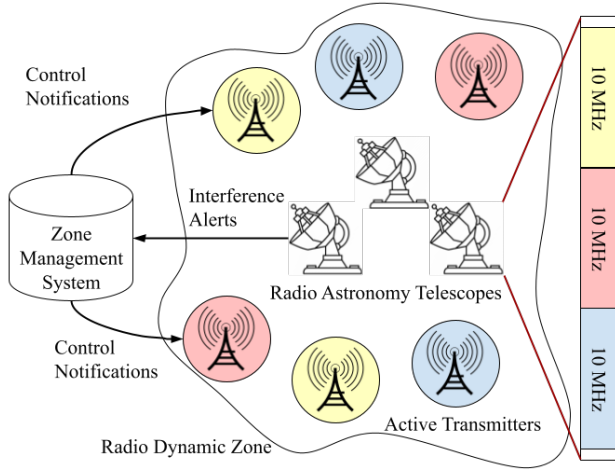
Fig. 1. Example of spectrum sharing scenario in RDZ with radio astronomy and active transmitters with a ZMS.

propagation behavior, providing a more informed starting point. ASTRA can handle uncertainty in propagation modeling and transmissions that results in interference. Third, ASTRA accommodates RAS's interference constraints. Lastly, RAS observations often span wide frequency ranges. We expect transmitters to operate in narrower bands within the observing range. ASTRA reassigns interfering transmitters to alternate bands rather than revoking access, provided interference constraints are not violated. This iterative reallocation mitigates interference while increasing spectrum utilization. ASTRA can adapt to environmental changes and dynamic transmitter behavior; however, we do not consider uncooperative interference sources.

To enable real active-passive spectrum coexistence, we develop the first RDZ testbed at a radio astronomy facility, the Hat Creek Radio Observatory (HCRO) [13]. Our deployment serves as a proof-of-concept, demonstrating a practical solution for managing spectrum for over-the-air experiments. Leveraging OpenZMS [7], an open-source automated spectrum management platform, we implement ASTRA to dynamically allocate spectrum to test transmitters, enabling opportunistic use while protecting sensitive telescopes from harmful interference. We highlight key OpenZMS services and features that we develop for RAS operations at the HCRO-RDZ.

To comprehensively evaluate our approach, we simulate the spectrum-sharing scenario between RAS and cellular users in RDZs of varying sizes. We examines the trade-off between spectrum utilization in the RDZ and interference at RAS. ASTRA maintains interference at RAS below acceptable thresholds, responding to interference within 105 seconds while allowing spectrum access for up to 64.6% of transmitters.

In summary, we outline a spectrum-sharing scenario in an RDZ to enable coexistence between passive RAS and active transmitters. We propose and deploy the ASTRA framework to coordinate spectrum access in the HCRO-RDZ. Finally, we evaluate the trade-off between minimizing interference at RAS and maximizing spectrum utilization in large RDZs.

II. Spectrum Sharing Scenario

RDZs are envisioned as a space for a diverse range of services and applications, from long-term spectrum use (years) to short-term, opportunistic access (minutes to months). To highlight the need for careful spectrum management, we outline the key characteristics and interference constraints of radio astronomy services (RAS) and discuss the operational requirements and expected behavior of RDZ transmitters.

A. Radio Astronomy Service

Radio astronomy is essential for expanding our understanding of the universe. While certain frequency bands are allocated for RAS, observations often extend beyond these bands, as targeted frequencies evolve over time. Radio telescopes, designed to detect faint signals as low as -206 dBm, are highly susceptible to interference from sources up to 100 km away [14]. Their instantaneous bandwidth, or *observing range*, can span several GHz. Observation sessions vary from minutes for transient events to hours or days for long-term monitoring [15]. Interference is often identified only during post-processing, leading to data loss and reduced sensitivity [16]. To mitigate this, facilities are developing real-time interference detection systems [10]–[12]. Acceptable interference is strictly limited to under 2% of total observing time from a single system and below 5% from all sources combined [17].

B. Active Users in RDZs

RDZs are expected to have a crucial role in current and next-generation cellular networks [6]. These zones enable testing of special transmitters, such as directed energy systems, high-power microwave transmitters [18], and experimental radio technology [5]. RDZ transmitters, particularly for cellular or experimental use, require less bandwidth than RAS. We assume transmitters request a contiguous band within RAS's observing range, specifying a 10 MHz primary band and optional secondary bands, as shown in Figure 1. Transmitters provide their location, operational parameters, and required transmission power range. We map RAS's acceptable interference limits–2% of observing time from one system–to the interference from each band allocated for transmitters.

III. Zone Management System

We utilize a Zone Management System (ZMS), shown in Figure 2, to manage spectrum access for RDZ transmitters to mitigate interference at RAS using the Adaptive Spectrum Tuning and Reactive Allocation (ASTRA) framework. While we do not consider a specific RAS interference detection system, we assume it reports interference during observations. The ZMS maintains operational data on radio telescopes and transmitters, and environmental and monitoring data. A Digital Spectrum Twin (DST) provides current and historical view of the spectrum using this data and propagation maps based on measurements and modeling [19]. While the DST estimates received power at radio telescopes, actual values may differ. The ASTRA framework, described next, adapts to imperfect modeling, dynamic transmission patterns, and changing environmental conditions.
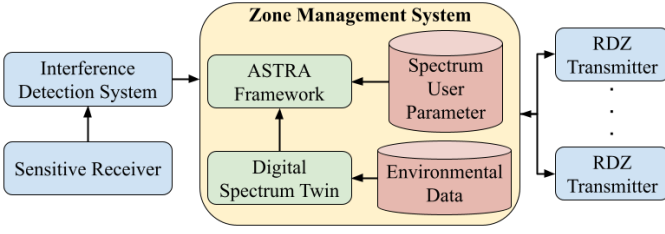
Fig. 2. ZMS components and interactions with RDZ users.

A. ASTRA Framework

ASTRA initializes transmit power for all transmitters requesting spectrum access. Thereafter, allocations are managed through the reactive interference management approach. When interference is reported, ASTRA revokes spectrum access from some transmitters. Transmission capabilities are gradually increased until interference reoccurs. Through this iterative process, ASTRA learns a safe power and spectrum allocation configuration for coexistence. ASTRA does not necessarily find the optimal configuration, rather it adapts and learns a safe sharing allocation configuration.

1) Initializing Power Allocation: Transmitters requesting spectrum access specify their power range and desired bands. We model the allocation problem to maximize the number of transmitters and optimize power allocation while adhering to RAS's interference constraints. Let N be the set of all transmitters, including those operating (O) in and requesting access (R) to the same band. The binary variable $z_i \in \{0,1\}$ indicates if transmitter i ($\in N$) is granted access. The total number of transmitters with spectrum access cannot exceed N

$$\sum_{i \in R} z_i + \sum_{i \in O} z_i \leq N. \tag{1}$$

Each transmitter i requests to transmit between the range P_i^{min} to P_i^{max}. The power allocated to transmitter i is represented by p_i. Access is granted if p_i is non-zero and within the requested range and denied if $p_i = 0$, i.e.,

$$P_i^{min} \cdot z_i \leq p_i \leq P_i^{max} \cdot z_i. \tag{2}$$

The DST calculates the expected path loss q_i from each transmitter to the radio telescopes, including those already operating. Total received power at RAS must remain below the interference threshold P_T such that

$$\sum_{i \in R} (p_i - q_i) + \sum_{i \in O} (p_i - q_i) \leq P_T. \tag{3}$$

The objective is to maximize the number of transmitters with access and their allocated transmit power

$$\text{Maximize} \sum_{i \in R} z_i + \epsilon \sum_{i \in R} p_i \tag{4}$$
$$\text{Subject to: } (1) - (3),$$

where ϵ is a small positive value that prioritizes maximizing the number of transmitters with access over their allocated power.

We model this optimization problem as a Mixed-Integer Linear Programming (MILP) problem and solve it using the well-known branch-and-bound method. This optimization step provides an initial allocation based on expected signal propagation but does not account for temporal or spatial variations. To address this limitation, we use a best-effort reactive approach to iteratively manage spectrum access.

2) Reactive Interference Management: ASTRA ranks transmitters by their interference potential in an *interferers list*, which is based on expected propagation behavior obtained from the DST. Hence, the accuracy of the interferers list depends on the DST's accuracy.

In response to observed interference, the ZMS instructs transmitters on the interferers list to pause spectrum use in the shared band. While interference continues, the ZMS updates the interferers list and further reduces spectrum use. Once interference stops, transmission capabilities are gradually increased, starting with those most recently paused. Over time, ASTRA refines and learns a safe sharing estimate of transmitters likely to cause harmful interference.

ASTRA updates the safe sharing estimate c when no interference is reported, recording the number of users sharing the band without causing interference. This estimate is used to identify transmitters previously known to cause interference. The number of transmitters with spectrum access at time t is denoted by n. When no interference is observed, we compute an exponentially weighted moving average (EWMA) of both the mean (μ_t) and the variance (σ_t) of n as

$$\mu_t = (1 - \alpha) \cdot \mu_{t-1} + \alpha \cdot n, \tag{5}$$
$$\sigma_t = (1 - \beta) \cdot \sigma_{t-1} + \beta \cdot |n - \mu_t|, \tag{6}$$

where α and β are weighting parameters. The safe sharing estimate c, calculated as $\mu_t - \sigma_t$, represents the lower bound of the weighted average. This estimate tracks historic interferes and converges towards the largest safe set of transmitters.

When revoking access from potentially interfering transmitters, ASTRA first determines the size of the interferers list (n_I) using the safe sharing estimate c. If interference persists, additional revoke operations are performed as described in Algorithm 1. We enforce two interference thresholds: I_T, the total acceptable interference threshold across all bands, and I_B, the per-band threshold. Duration of interference in each band and across all bands during the observation session is recorded in I_b and I_t, respectively. We define interference capacity as the ratio of observed interference duration to the interference threshold. As shown in Algorithm 1, the interferers list size increases proportional to I_Δ, the higher interference ratio (or lower remaining interference capacity). This step ensures interference remains below both thresholds.

To account for changes in the RDZ, in the absence of interference, ASTRA gradually increases transmissions. When I_t and I_b are sufficiently below thresholds I_T and I_B, respectively, ASTRA enhances spectrum reuse through three steps shown in Algorithm 2. First, a set of transmitters most recently revoked are reassigned spectrum access, inversely proportional

Algorithm 1 Update Interferers ($users, interferersList, c$)

1: **if** $length(users) > c$ **then**
2: $\quad n_I \leftarrow length(users) - c$
3: **else**
4: $\quad I_\Delta \leftarrow \max(I_t/I_T, I_b/I_B)$
5: $\quad n_I \leftarrow length(users) \cdot I_\Delta$
6: **end if**
7: $interferersList \leftarrow \text{sort}(users, n_I)$
8: $users \leftarrow \text{revoke}(interferersList)$

---

to I_Δ. Their transmit power is set to the minimum of their most recent or optimized power allocation (Section III-A1), provided it is non-zero. Next, if sufficient interference capacity exists, allocated power for select transmitters operating below their requested power is increased. The number of transmitters in this set is proportional to the remaining interference capacity. Finally, if sufficient interference capacity remains, transmitters identified as causing interference in other bands, in the *deferred list*, are iteratively added. Their transmit power is set to the lower of their optimized power allocation (Section III-A1) or their minimum power request, provided it is non-zero. This step maximizes spectrum reuse while adhering to interference thresholds.

Algorithm 2 Increase Allocation ($users, interferersList$)

1: $I_\Delta \leftarrow \max(I_t/I_T, I_b/I_B)$
2: **if** $interferersList$ is not empty **then**
3: $\quad n_I \leftarrow length(users) \cdot (1 - I_\Delta)$
4: $\quad users \leftarrow \text{reassign}(\text{reverse}(interferersList, n_I))$
5: **end if**
6: **if** $n_I > length(interferersList)$ **then**
7: $\quad n_P \leftarrow n_I - length(interferersList)$
8: $\quad \text{increasePower}(users, n_P)$
9: **end if**
10: **if** $n_P > length(users)$ **then**
11: $\quad n_R \leftarrow n_P - length(users)$
12: $\quad users \leftarrow \text{reassign}(deferredList, n_R)$
13: **end if**

IV. RADIO DYNAMIC ZONE AT HAT CREEK RADIO OBSERVATORY

We develop an experimental testbed at the Hat Creek Radio Astronomy Observatory (HCRO) to demonstrate our spectrum-sharing scenario. We use OpenZMS [7], an automated spectrum management platform, to regulate spectrum access in the zone. This section describes the test transmitters and spectrum monitors that we deploy on-site and highlights key OpenZMS services that we develop to support the testbed experiments.

A. RDZ testbed

Our RDZ testbed includes three spectrum participants – radio telescopes, spectrum monitors, and test transmitters, as shown in Figure 3. The area shown spans approximately 1 km x 0.7 km. HCRO hosts the Allen Telescope Array,

consisting of 42 radio astronomy dishes, each 6.1 m in diameter. To monitor interference, we use six SDR-based spectrum monitors, previously installed around the facility [10], which continuously scan the spectrum and report interference using spectral kurtosis analysis [20]. Additionally, for this experiment, we build and deploy three SDR-based nodes to operate as transmitters in the RDZ, co-located with spectrum monitors due to limited locations with power and Ethernet access. OpenZMS manages spectrum access to these test transmitters, using spectrum monitors to detect interference at RAS.
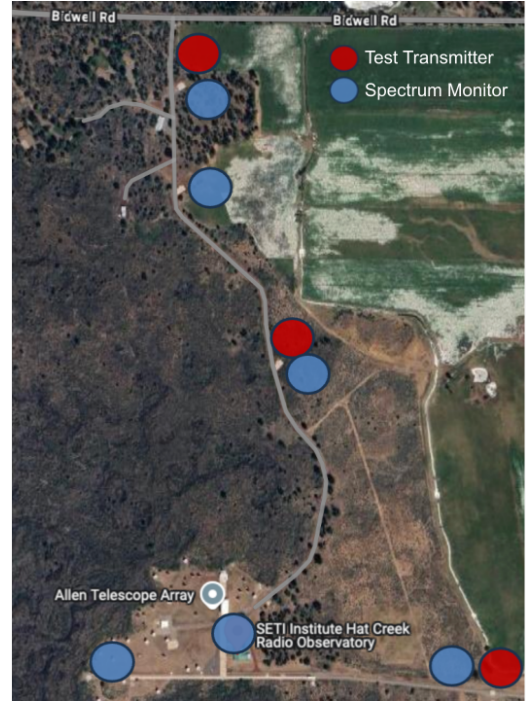

Fig. 3. Spectrum participants of the RDZ testbed developed at HCRO.

B. Experiment Workflow with OpenZMS

Figure 4 illustrates the interaction between OpenZMS and the zone participants. This figure presents an abbreviated view of the core OpenZMS components that we use in our HCRO deployment (see [7] for a detailed description of OpenZMS). We model the two spectrum stakeholders as OpenZMS *Elements* (similar to cloud tenants), each with distinct spectrum roles, priorities, and constraints. Participants (administrators, daemons) interact with OpenZMS via its web UI or RESTful APIs (the Zone Element Abstraction Layer, *ZeAL*). In our setup in this paper, the *HCRO* element contains the radio telescopes and the spectrum monitors. The *Active Users* element includes the test transmitters. The spectrum participants within these elements can perform different roles – *spectrum providers, monitors, and consumers*. We develop the following end-to-end workflow:

1) Radio astronomy, as the spectrum provider, specifies the permissible sharing frequency range and policy guidelines for secondary use to the OpenZMS *Zone Management Controller (ZMC)*.

2) Test transmitters, as spectrum consumers, request access via spectrum *Grants*. If the requests comply with policy constraints, the ZMC grants them lower-priority access.
3) When operating, radio telescopes act as spectrum consumers and hold the highest priority spectrum grants.
4) Spectrum monitors periodically update the *DST* with monitoring and interference observations. The DST analyzes and forwards these to the *Alarm* service.
5) The Alarm service processes interference data and recommends corrective actions to grants based on ASTRA to the ZMC. The ZMC processes the recommendations and updates the grants based on the suggested actions.
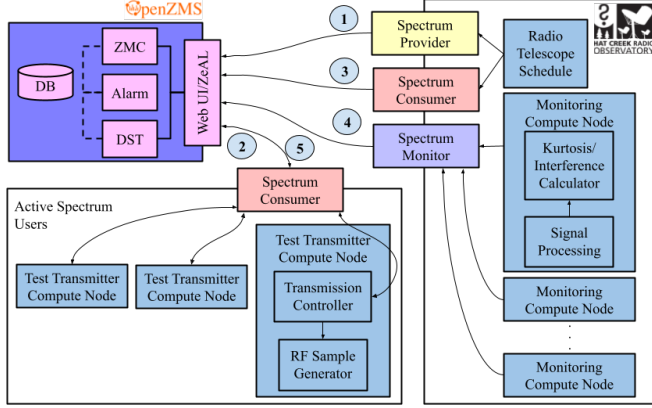

Fig. 4. Experiment setup and workflow for HCRO-RDZ testbed and OpenZMS, test transmitter, and spectrum monitors' software stacks.

We operate the three test transmitters simultaneously at 910 MHz. The monitors detect their signals, as displayed in the monitoring dashboard in Figure 5. When interference is reported, OpenZMS modifies spectrum grants, pausing one transmitter and reducing the transmit power of another, while leaving the third unchanged, as shown in Figure 6. This is reflected in the monitor's observations as one transmitter turns off and one lowers power, see yellow and blue observations, respectively, in Figure 5. Due to the transmitter locations and power constraints, reassigning these transmitters to another band within the observing range also results in interference.
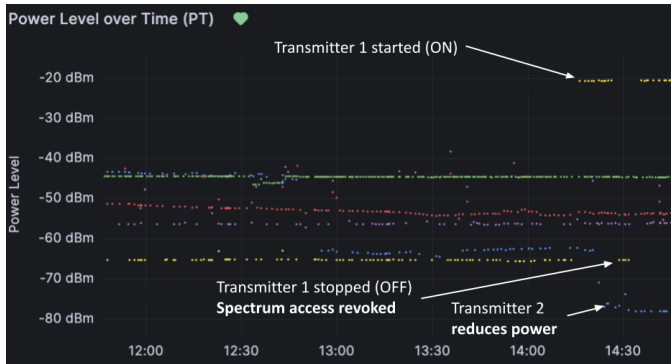

Fig. 5. Spectrum monitoring dashboard with power observed by each monitor showing one transmitter turning off and one reducing power.
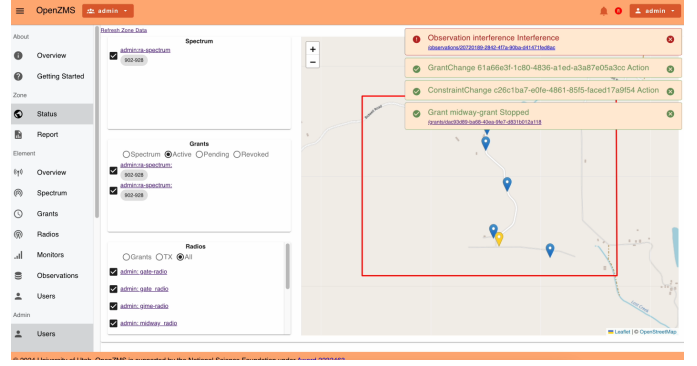

Fig. 6. OpenZMS frontend with interference notifications and corrective test transmitter grant modifications.

C. RDZ Test transmitters

In this section, we describe the SDR-based transmitter nodes that we build and deploy on-site and the software we develop to program the SDRs and interface with OpenZMS.

1) Hardware: Each test transmitter node consists of a Taoglas I-bar omnidirectional antenna connected to an SDR system housed in a weatherproof junction box shown in Figure 7. The box contains a JRE Test 0709 RF-shielded enclosure (3.5" x 6" x 8.5") to minimize electromagnetic interference (EMI) as shown in Figure 8. Inside the enclosure, an NI B205-mini SDR handles RF signal generation, controlled by a Raspberry Pi 4B. Network connectivity is provided by a 1 Gbps UMC-GA1F1T fiber-to-copper media converter, linking the SDR node to the local network via optical fiber. To restrict unwanted transmissions, a Mini-Circuits SLP-1000+ low-pass filter is included in the RF chain, connected to the antenna. Each SDR node's output power is restricted to 12 dBm using attenuators to protect sensitive on-site equipment. Figure 9 shows the block diagram of our test transmitter at HCRO.

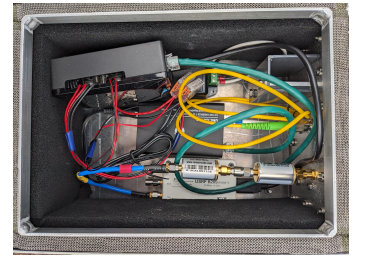Fig. 7. Our RDZ test transmitter installed at HCRO.

Fig. 8. SDR-based test transmitter node in EMI enclosure.

2) Software: Our software components reside on the Raspberry Pi, which powers and controls the SDR and transfers data to the host via a USB connection. To prevent unwanted emissions, we permanently disable the Wi-Fi and Bluetooth modules by blacklisting them with *rfkill*.

Our test transmitter software consists of two components: (1) Transmission Controller, that interfaces with OpenZMS to send operational control messages. It requests spectrum grants
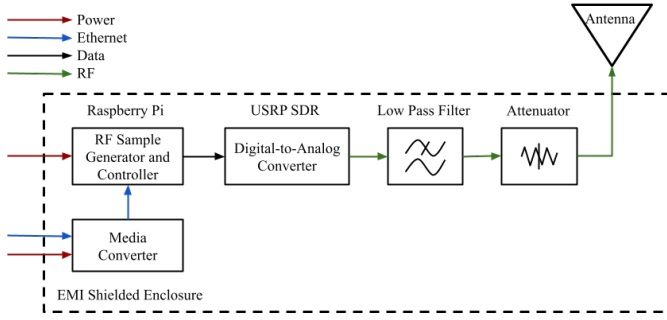
Fig. 9. Block diagram of our test transmitters installed at the HCRO-RDZ.

and monitors grant status changes to update the transmission state (e.g., starting or stopping transmissions or adjusting transmit gain). It also automatically logs transmission parameters, including start/stop times, signal type, transmit gain, and transmitter node metadata, for manual verification by testbed operators. (2) RF Sample Generator that provides the digital input to the SDR using USRP Hardware Drivers (UHD) Python 3 APIs. It enables the transmitter nodes to generate continuous wave and BPSK-modulated signals for specified durations, operating under the controller's commands.

D. RFS Spectrum Monitors

Unlike the transmitters that we build for our RDZ testbed, we do not build any new monitors but instead leverage the existing spectrum monitoring infrastructure. The hardware design, calibration procedure, and noise temperature comparisons for these sensors are detailed in [10]. Next, we describe the software components of the SDR-based RF baseline Sensors (RFS) that we develop for collecting, processing, and storing RF IQ data, as well as interfacing with OpenZMS for interference reporting.

1) RFS Software & database: The RFS software stack we develop and host on a Raspberry Pi 4B uses the UHD Python API for SDR control and I/Q sample collection. We manage automated data backup and error notifications via *rsync* and email utilities. We use a cron-based monitoring system to check logs and report status. We store key metrics, including signal power, frequency occupancy, and interference events, in a time-series database with metadata such as sensor location, timestamp, and configuration parameters.

2) OpenZMS monitor client: We develop the monitoring client to connect the RFS database to OpenZMS, processing RF survey data to potential interference events. It maintains exponentially weighted moving averages of power, and computes kurtosis over 200,000 data points, tracking statistics per frequency band for band-specific detection. For each measurement, the client computes the mean and standard deviation of both power and kurtosis measurements. Measurements exceeding three standard deviations trigger interference flags, requiring consecutive occurrences (default value 2) to minimize false positives. This helps filter out transient anomalies while ensuring reliable detection of sustained interference events. Reports are formatted in DST JSON and sent to OpenZMS

via REST API, including timestamps, frequency, power levels, kurtosis, and metadata for interference attribution.

E. OpenZMS Implementation for HCRO-RDZ

OpenZMS is implemented in Golang and provides user-facing APIs via a RESTful JSON interface with role-based access control (RBAC). Internal service communication uses gRPC APIs and publish/subscribe event streams, ensuring high-throughput and reactive workflows. We build upon three core OpenZMS services - the Zone Management Controller, the Digital Spectrum Twin, and the Alarm service, to enable our reactive sharing approach for HCRO as described below.

1) Zone Management Controller (ZMC): The ZMC exposes spectrum provider and consumer APIs for element users to interface with OpenZMS. It hosts the spectrum scheduler, which allocates spectrum using a *Grant* abstraction, performing conflict checks based on radio characteristics, spectrum policies, and coexistence policies. The ZMC interfaces with the DST and Alarm services for spectrum access decisions.

We encode coexistence policies, defined by the radio astronomy element acting as the *spectrum provider*, for spectrum management in the ZMC, specifying parameters like frequency range, duration, maximum power, and per-element consumer policies (maximum grant priority, grant exclusive-access mode, conflict tolerance, and more). These policies specify how multiple users can be granted access based on interference constraints and priority. Interference constraints are specified as *static* or *runtime*. Our ZMC scheduler analyzes static constraints to determine a priori conflicts with existing grants before approving a new grant request. Runtime constraints define limits on interference detected during grant "runtime" by spectrum monitors. Our Alarm service updates and tracks runtime constraints.

The radio astronomy element, acting as a spectrum consumer, requests high-priority grants from OpenZMS for telescopes, specifying runtime constraints like acceptable interference duration and thresholds. Our test transmitters request low-priority grants. We ensure that these low-priority grants do not violate the higher-priority radio astronomy grant constraints to operate in the declared frequency range.

2) Digital Spectrum Twin (DST): The OpenZMS DST contains RF propagation simulations and observations reported by spectrum monitors via queryable APIs. In our deployment, the DST determines the expected signal propagation for the $2 \times 2\ km^2$ HCRO area using digital terrain maps and the TIREM model [21]. Prediction query APIs are utilized by the ZMC's scheduler and the Alarm service (described below) to identify potential interferers. The DST also processes spectrum monitoring reports containing timestamps, frequencies, observed power, and impacted grants (if verified). For our experiment, we categorize reports as *Interference* that indicate harmful, unexpected interference, or as *Observation*, which are values of observed power below the interference threshold.

3) Alarm Service: We develop the Alarm service to handle violations of the radio astronomy spectrum and grant constraints. Our Alarm service monitors DST reports for viola-

tions. Upon receiving an *Interference* report, the Alarm service verifies constraint policies and identifies potential interferes among lower-priority grants in the same band using ASTRA. It recommends grant modifications to the ZMC, specifying either power reduction or access revocation. For *Observation* reports, the Alarm service updates coexistence parameters, enabling the ZMC to reassign or resume grants for lower-priority consumers when possible. To implement power initialization, we utilize the Golp Golang wrapper for LPSolver [22]. We scale linear power values to prevent floating-point underflow and aggregate these for the MILP solver.

V. Large-Scale Simulation

We simulate large-scale HCRO-RDZs to evaluate ASTRA beyond the physical limitations of the deployment described above. Specifically, we examine radio telescopes' susceptibility to long-distance interference from opportunistic cellular usage in the region around HCRO. In this section, we first model two types of spectrum users – the higher-priority incumbent radio astronomy user and lower-priority opportunistic cellular users. Next, we model the region surrounding HCRO. Last, we model the key components of the ZMS. We conclude by presenting the results of our simulation.

A. Radio Astronomy Users

We model radio astronomy operations in the 1.4-1.43 GHz band, crucial for studies of hydrogen line emissions and large-scale sky surveys [15]. The telescope array is located at the center of the simulated map (Figure 10). The interference threshold is -180 dBm/10 MHz. Aggregate power above this level causes harmful interference. Observation sessions last 30 minutes to 24 hours. The acceptable interference period must not exceed 2% and 5% of the observation session's duration in each 10 MHz band and across the entire observing range, respectively. We do not assume any particular method of detecting interference and assume that RAS has the capability to detect interference accurately during observations.

B. RDZ Cellular Transmitters

The RDZ transmitter deployments span areas ranging from $4 \times 4\ km^2$ to $8 \times 8\ km^2$, located approximately 50 km from the observatory. The transmitters model a realistic deployment of cellular users operating opportunistically in shared bands [23]. The simulation area is divided into equal-sized grids of $1 \times 1\ km^2$, with transmitters randomly distributed within each grid. Varying density within each grid denotes different numbers of users in the zone. To examine diverse sizes, we implement four transmitter densities – 3, 5, 7, and 10, in each grid for both RDZ area sizes. The heights and power levels of the transmitters are also based on [23]. Each transmitter requires a 10 MHz band (primary band) or can optionally be reallocated to one of two secondary 10 MHz bands within the 30 MHz observing range. We model the transmitter activity as an ON/OFF process reflecting cellular user behavior [24]. We refer to this type of transmitter activity as *dynamic operations*. We also model another scenario where all transmitters operate simultaneously at full power. We refer to this scenario as *peak operations*.

C. Geographic Region And Signal Propagation Models

We utilize the USGS 1/3 arc-second digital elevation map [25], spanning $100\ km \times 100\ km$ with a $10\ m$ resolution, shown in Figure 10, to capture the topography surrounding HCRO. We simulate signal propagation by calculating point-to-point path loss between each transmitter and telescope using the TIREM model [21] utilizing geographic and environmental characteristics. The environmental characteristics, including the refractive index, conductivity, and humidity, are obtained from [25]. The sum of received power from all transmitters determines aggregate interference at the telescopes.
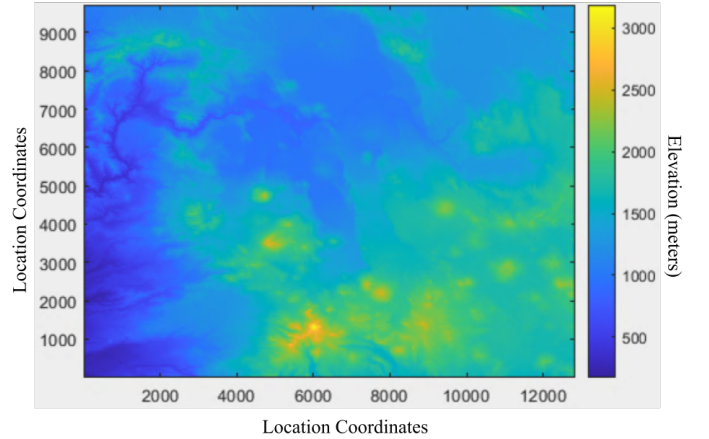

Fig. 10. Digital elevation map around HCRO.

D. ZMS Components

We simulate the DST and the ZMS's interactions with radio astronomy and cellular transmitters to reflect realistic operations and implement ASTRA's power initialization and reactive algorithms in our simulation.

1) DST Simulation: The DST informs spectrum allocation decisions in the RDZ. While the TIREM propagation model provides ground truth for signal propagation in our simulation, real-world DSTs often exhibit discrepancies with the ground truth. We introduce realistic errors into the DST's path loss predictions to reflect this.

The DST path loss (PL) deviates from the ground truth, mirroring discrepancies observed in measurement campaigns in diverse locations [26]. We model shadow-fading errors as a log-normal random variable with standard deviation (σ) derived from empirical data.

TIREM captures spatial correlation in path loss predictions, while added noise accounts for measurement-model differences. Combining these aspects provides a more realistic representation of the uncertainty. The combined path loss is expressed as $PL_{DST} = PL_{TIREM} + X_\sigma$, where X_σ is the log-normal variable representing DST uncertainty relative to ground truth.

2) Allocation Initialization: We use the open-source Python PuLP package to solve the MILP problem to optimize initial transmitter allocations. The aggregate interference constraint (Equation 3) is modeled as a linear additive constraint by converting all power values to the linear scale.

3) Reactive Framework: Since the optimizer relies on noisy path loss values from the DST, the allocation may not prevent interference. The reactive algorithms address subsequent interference and modify spectrum allocations accordingly. The ZMS tracks multiple interference metrics to ensure compliance with protection thresholds in-band and across all the bands. The weights α (Equation 5) and β (Equation 6) used to compute the safe sharing estimate are set to 0.125 and 0.25, respectively, based on simulation results.

E. Performance Evaluation

We present the interference and spectrum utilization results from our simulation comparing ASTRA to the basic framework in [6]. To establish the minimum bound for any reactive approach, we consider a baseline approach where the ZMS revokes access from all transmitters upon interference detection. Each scenario covers one simulated day with a 1-minute granularity. We present results using the three approaches (ASTRA, basic, and baseline) by averaging results over 100 simulations for each case we consider – for RDZ sizes ranging from 48 to 640 transmitters, under peak and dynamic operations. Recall from Section V-B that peak operation corresponds to all transmitters transmitting simultaneously at maximum power, and dynamic operation uses an ON/OFF model. **Figures 11-18 show dashed lines for dynamic operations and solid lines for peak operations.**

1) Acceptable Interference Period at RAS: The interference period measures the percentage of time RAS experiences interference during an observation session. Figure 11 shows the mean of the total interference period across (y-axis) for different RDZ sizes (x-axis). The baseline approach achieves the best performance with a reactive approach, with a lower bound of 0.32% of the observation session. All approaches ensure the interference period remains below the acceptable threshold, as the ZMS revokes transmitter access when limits are exceeded. Under peak operations, ASTRA exhibits similar interference to the basic approach (4.97% vs. 4.92%). For dynamic use, ASTRA maintains interference below 4%, well under the 5% threshold, indicated by the dotted black line.

Figure 12 depicts the mean interference period per 10 MHz band. The baseline behavior mirrors Figure 11. ASTRA results in slightly lower interference than the basic approach in peak use. The basic approach achieves 1.18% interference for dynamic use in the worst case, compared to ASTRA's 1.41%. These minor differences keep all approaches within the 2% threshold denoted by the dotted black line.

2) Interference Response Time: This metric captures the system's response time to interference by measuring the duration from interference detection to resolution. Figure 13 plots the average response time for the RDZ sizes considered. The response time remains under 2.4 minutes for all scenarios.

ASTRA outperforms the basic approach with peak operations, reducing response time by 30 seconds on average, except for the 160 transmitter case, where basic is faster by 15 seconds. It is unclear why the difference is reversed in this case. The crucial takeaway is that the response time for ASTRA is consistently under 1.8 minutes with peak use. For dynamic use, ASTRA achieves a consistent 70-second average response time, while the time with the basic approach slows as transmitters increase, lagging ASTRA by 40 seconds.

3) Interference Events at RAS: We analyze the frequency of interference experienced by RAS. Figure 14 shows the average number of events. Although ASTRA resolves interference faster, it results in more events than the basic framework. The difference is minor for peak use, with ASTRA averaging 5 additional events. Under dynamic use, ASTRA maintains a consistent average of 46 events, while the basic framework shows a notable decline in events as transmitters increase.

4) Spectrum Reuse by Transmitters: Figure 15 shows the spectrum utilization as the fraction of transmitters allocated spectrum during RAS operations. Shaded regions represent the standard deviation of the utilization. Dynamic operations perform worse due to unpredictable usage patterns, with interference events reducing allocations. ASTRA consistently outperforms the basic approach, achieving up to 64.6% utilization and improving spectrum access by up to 2.6 times. ASTRA supports up to 134 transmitters, compared to 56 with the basic framework. Even under peak use, ASTRA's lowest utilization exceeds the basic approach's best, except for the 48-transmitter scenario. ASTRA achieves 0.85 times higher spectrum reuse for dynamic operations than the basic framework.

5) Coverage Area Granted to RDZ Users: We analyze spectrum allocations for transmitters using ASTRA by comparing the allocated coverage area to the area requested by all transmitters. Coverage area is defined by map pixels where the received signal exceeds the -110 dBm benchmark of minimum signal for cellular use [27]. Figure 16 shows the cumulative density function (CDF) of the fraction of transmitters to the fraction of allocated coverage area to the requested area. We only show the coverage area for **peak operations**. A higher fraction signifies that the allocated coverage closely matches the request, with the maximum value signifying that requests were fully met. A steeper slope suggests that more transmitters received smaller portions of their requested area. Larger RDZs generally have fewer transmitters obtaining full coverage. In the 48-transmitter RDZ, 35% of transmitters receive no coverage area. Transmitters with no coverage increases to 67.8% for the 640-transmitter RDZ. On the other end, 45.8% of transmitters in the 48-transmitter RDZ get their complete coverage request, compared to only 11.7% in the 640-transmitter RDZ. An incremental increase in allocated coverage across RDZ sizes suggests that partial allocations are contributing to the higher spectrum reuse in Figure 15.

6) Continuous Spectrum Access: We track the duration of uninterrupted spectrum access assigned by ASTRA and the basic framework for all transmitters. Figure 17 compares the CDF of transmitters versus spectrum access duration for
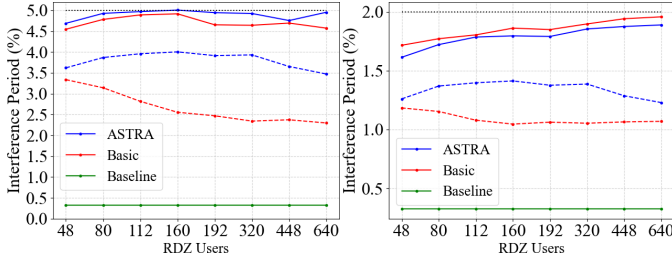
Fig. 11. Interference period observed at RAS across all RDZ bands.

Fig. 12. Interference period observed at RAS in each 10 MHz band.
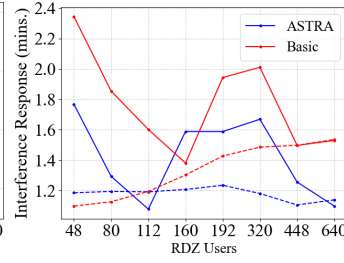
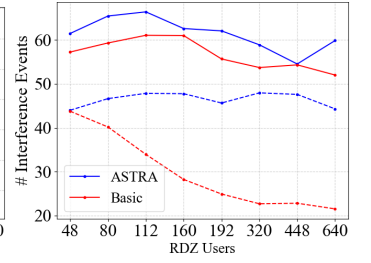Fig. 13. Average time taken to stop interference.

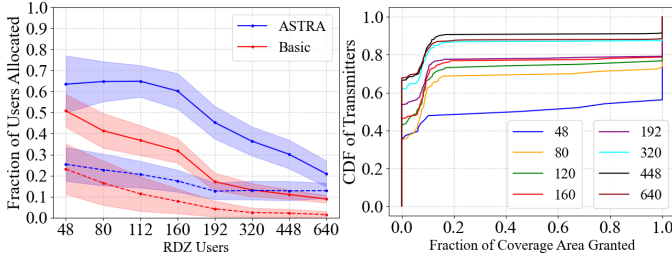Fig. 14. Mean number of interference events observed at RAS.

Fig. 15. Average number of transmitters with spectrum access.

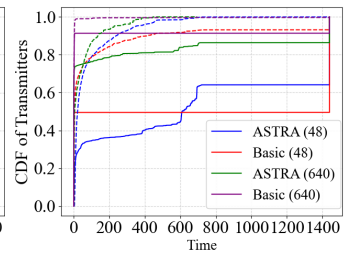Fig. 16. Distribution of coverage area granted to transmitters.

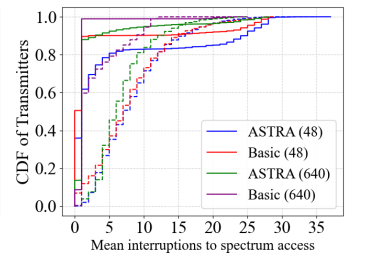Fig. 17. Average duration of continuous spectrum access to transmitters.

Fig. 18. Number of interruptions to spectrum access for transmitters.

transmitters in two RDZ sizes: 48 and 640 transmitters. We exclude other RDZ sizes as their performance lies between these two cases. In the 48-transmitter RDZ, the basic approach shows that 53.15% of transmitters never have spectrum access, while the rest experience uninterrupted access. In contrast, CDF with ASTRA rises gradually, indicating longer access periods, with 64.6% of transmitters with spectrum access and 35.84% of transmitters maintaining continuous access for the entire duration. With 640 transmitters, ASTRA provides continuous access for 12.5% of transmitters, compared to 7.6% with the basic approach. Both approaches yield shorter access periods under dynamic operations. ASTRA does not allocate spectrum for more than 700 minutes. The basic approach only provides continuous spectrum access to 4.1% of transmitters in the 48-transmitter RDZ. In the 640-transmitter RDZ, ASTRA allocates a maximum of 387 minutes of access, whereas the basic approach provides no spectrum access.

7) Interruptions to Spectrum Access: Figure 18 shows the frequency of spectrum access interruptions for two RDZ sizes: 48 and 640 transmitters. Under peak operations, the basic approach never provides access to 50.5% of transmitters. In the 640-transmitter RDZ, almost all transmitters experience immediate interruptions after gaining access. In contrast, ASTRA results in no more than 27 interruptions per user. Under dynamic use, interruptions are fewer overall. For the 48-transmitter RDZ, both approaches perform similarly, but with 640 transmitters, ASTRA exhibits fewer interruptions, as shown by a steeper rise. With peak operations, the curves rise quickly, indicating frequent interruptions for more transmitters, whereas with dynamic operations, interruptions are more evenly distributed. Across all scenarios, ASTRA consistently results in fewer interruptions, making it more reliable.

8) Summary of Results: The comparison between AS-TRA and the basic approach highlights trade-offs between spectrum utilization among transmitters and interference at RAS. ASTRA maintains interference within acceptable limits, though slightly higher than the basic approach. It prioritizes rapid mitigation, leading to shorter, more frequent interference events, which RAS can manage effectively through excision. ASTRA is more effective in high-density, variable-use scenarios, consistently achieving better spectrum utilization through partial allocations. However, ASTRA repeatedly interrupts the same transmitters when interference is observed. In contrast, the basic approach results in lower interference due to frequent revocations, leading to lower utilization in large RDZs.

VI. RELATED WORK

In our deployment of the HCRO-RDZ, the monitors are co-located with the transmitters, which is unlikely for most RDZs. In [28], RDZs are bounded areas monitored by spectrum sensors for comprehensive coverage. They address optimal sensor placement with autonomous aerial and ground sensors, using Kriging-based methods to construct and validate 3D spectrum usage maps. The power allocation scheme in [29] enables sharing between RAS and 5G to maximize transmit power uniformly across all base stations. However, it relies on static models that do not adapt to temporal or spatial changes and only address out-of-band interference. In [30], spectrum licenses are likened to property rights for static allocations. A protocol for passive users to publish their band usage is introduced in [31], prompting active systems to pause operations. The watermarking scheme in [32] identifies transmitters interfering with RAS. Similarly, Radio Quiet Zones around radio astronomy facilities restrict transmission for over 100

km away [8]. These approaches mitigate interference to RAS but do not enable coexistence with active transmitters. The beacon-based notification system in [33] prevents satellite interference to RAS using path loss models to determine interference probability and must ensure that the beacons do not harm the sensitive telescopes while being able to reach the satellites. Methods to correct data corrupted in RAS observations are proposed in [34]; however, they do not consider multiple sources of RFI. Unlike existing work, we introduce a reactive framework for minimizing interference at RAS and maximizing spectrum utilization among active users in the RDZ that adapts to changes in the zone. Existing spectrum-sharing solutions require all potential interferes, up to 100 km away, to vacate the band within one minute [1], [2]. We show that ASTRA effectively responds to interference within two minutes while allowing transmitters to operate within less than 50 km of RAS. Furthermore, we develop the first RDZ testbed at a radio astronomy facility to demonstrate the practicality of our reactive framework.

VII. Conclusion

We proposed the Adaptive Spectrum Tuning and Reactive Allocation (ASTRA) framework to enable safe coexistence between radio astronomy telescopes and RDZ transmitters by leveraging interference detection. We also developed the first RDZ testbed at Hat Creek Radio Observatory (HCRO) to demonstrate ASTRA, which effectively manages active transmitters in an over-the-air experiment. Our RDZ testbed can be utilized to conduct further coexistence experimentation. We demonstrated that ASTRA effectively manages harmful interference at radio astronomy telescopes while supporting a large number of dynamic, active transmitters located over a large area in a simulated RDZ.

Acknowledgment

References

[1] M. H. Dortch, "Amendment of the Commission's rules with regard to commercial operations in the 3550-3650 MHz band," Federal Communications Commission, Order on Reconsideration and Second Report and Order FCC 16-55, 2016.

[2] ——, "Unlicensed use of the 6 GHz band," Federal Communications Commission, Report and Order and Further Notice of Proposed Rulemaking FCC 20-51, 2020.

[3] ——, "Expanding flexible use of the 3.7 to 4.2 GHz band," Federal Communications Commission, Report and Order and Order of Proposed Modification FCC 20-22, 2020.

[4] A. Davidson, "National spectrum strategy implementation plan," NTIA, Tech. Rep., 2024.

[5] M. Zheleva, C. R. Anderson, M. Aksoy, J. T. Johnson, H. Affinnih, and C. G. DePree, "Radio dynamic zones: Motivations, challenges, and opportunities to catalyze spectrum coexistence," IEEE Communications Magazine, 2023.

[6] A. Sarbhai et al., "Reactive spectrum sharing with radio dynamic zones," in IEEE International Symposium on Dynamic Spectrum Access Networks, 2024.

[7] D. Johnson et al., "POWDER-RDZ: Prototyping a radio dynamic zone using the POWDER platform," in IEEE International Symposium on Dynamic Spectrum Access Networks, 2024.

[8] International Telecommunication Union, "Characteristics of radio quiet zones," Report ITU-R RA.2259-1, Tech. Rep., 2021.

[9] B. W. Fabio Giovanardi, Vincenza Tornatore and P. Bolli., "Compatibility studies between radio astronomy and three upcoming technologies," National Institute for Astrophysics, Tech. Rep., 2023.

[10] S. Tschimben et al., "Testbed for radio astronomy interference characterization and spectrum sharing research," in IEEE Aerospace Conference, 2023.

[11] National Radio Astronomy Observatory. (2023) National radio dynamic zone (NRDZ). [Online]. Available: https://info.nrao.edu/do/spectrum-management/national-radio-dynamic-zone-nrdz

[12] V. Prayag, G. Hellbourg, and M. Virgin, "Design of a mobile rfi monitoring station for dsa-2000 candidate sites surveys," in URSI Atlantic and Asia Pacific Radio Science Meeting, 2022.

[13] SETI Institute. (2024) Hat creek radio observatory, a seti institute research facility. [Online]. Available: https://www.seti.org/hcro

[14] International Telecommunication Unio, "Studies on compatibility of broadband wireless access (BWA) systems and fixed-satellite service (FSS) networks in the 3400–4200 MHz band," Tech. Rep., 2010.

[15] "Handbook on radio astronomy," International Telecommunication Union, Tech. Rep., 2013.

[16] T. E. Gergely, "Spectrum access for the passive services: the past and the future," Proceedings of the IEEE, 2014.

[17] D. DeBoer et al., "Radio frequencies: Policy and management," IEEE Transactions on Geoscience and Remote Sensing, 2013.

[18] T. Kidd, "National radio quiet and dynamic zones," in Information Technology Magazine. The Department of the Navy, 2018.

[19] G. D. Durgin, M. A. Varner, N. Patwari, S. K. Kasera, and J. Van der Merwe, "Digital spectrum twinning for next-generation spectrum management and metering," 2022.

[20] A. Mirhosseini, "High cadence kurtosis based RFI excision for CHIME," Ph.D. dissertation, University of British Columbia, 2020.

[21] M. A. Varner, T. A. Rodriguez, and G. D. Durgin, "RF coverage mapping of bistatic radio links using the terrain integrated rough earth model," in 16th European Conference on Antennas and Propagation, 2022.

[22] D. Sperger. (2024) Golp: a Golang wrapper for the LPSolve linear (and integer) programming library. https://pkg.go.dev/github.com/draffensperger/golp.

[23] W. Gao and A. Sahoo, "Performance impact of coexistence groups in a GAA-GAA coexistence scheme in the CBRS band," IEEE Transactions on Cognitive Communications and Networking, 2021.

[24] L. Csurgai-Horváth and J. Bitó, "Primary and secondary user activity models for cognitive wireless network," in Proceedings of the 11th International Conference on Telecommunications, 2011.

[25] OpenTopography. (2021) United States geological survey 3d elevation program 1/3 arc-second digital elevation model. https://doi.org/10.5069/G98K778D.

[26] C. R. Anderson, "An integrated terrain and clutter propagation model for 1.7 GHz and 3.5 GHz spectrum sharing," IEEE Transactions on Antennas and Propagation, 2022.

[27] K. Bechta, J. Du, and M. Rybakowski, "Rework the radio link budget for 5G and beyond," IEEE Access, 2020.

[28] S. J. Maeng, O. Ozdemir, Güvenç, and M. L. Sichitiu, "Kriging-based 3-D spectrum awareness for radio dynamic zones using aerial spectrum sensors," IEEE Sensors Journal, 2024.

[29] N. Jai, Y. Shi, W. Lou, L. DaSilva, and Y. Thomas Hou, "Out-of-band interference management to protect radio astronomy," in IEEE Military Communications Conference, 2024.

[30] M. B. Weiss, A. Palida, I. Murtazashvili, P. Krishnamurthy, and P. J. Erickson, "A property-rights mismatch approach to passive-active spectrum use coexistence," in IEEE international symposium on dynamic spectrum access networks, 2021.

[31] A. Palacios, D. Bronson, J. Backman, K. Warnick, and P. Lundrigan, "A versatile wireless network protocol for spectrum sharing with passive radio services." arXiv preprint, 2023.

[32] G. Hellbourg, N. Patwari, M. Weldegebriel, and N. Zhang, "Dynamic rfi management in radio astronomy using pseudonymetry," in United States National Committee of URSI National Radio Science Meeting, 2024.

[33] C. Ozturk, R. A. Berry, D. Guo, M. L. Honig, and F. D. Lind, "Reducing satellite interference to radio telescopes using beacons," in 2024 IEEE International Symposium on Dynamic Spectrum Access Networks (DySPAN), 2024, pp. 249–256.

[34] Z. Zou, X. Wei, D. Saha, A. Dutta, and G. Hellbourg, "Scisrs: Signal cancellation using intelligent surfaces for radio astronomy services," in *IEEE Global Communications Conference*, 2022.